An Enhanced Interface for Grid-connected PV Solar Systems

Ch. Swapan[1], D. Redya[2]

[1]Dept. of EEE, SreeDattha Institute of Engineering and Science, Hyderabad, India

Abstract - The penetration of photovoltaic (PV) solar power generation in distributed generation (DG) systems is growing rapidly. This condition imposes new requirements to the operation and management of the distribution grid, especially when high penetration levels are achieved. Under this scenario, the power electronics technology plays a vital role in ensuring an effective grid integration of the PV system, since it is subject to requirements related not only to the variable source itself but also to its effects on the stability and operation of the electric grid. This paper proposes an enhanced interface for the grid connection of PV solar systems. The relationship between output voltage components of each module and power generation is analyzed with the help of a newly derived vector diagram which illustrates the proposed power distribution principle. On top of this, an effective control system including active and reactive components extraction, voltage distribution and synthesization, is developed to achieve independent active and reactive power distribution and mitigate the aforementioned issue. Finally, a 3-MW, 12-kV PV system with the proposed control strategy is modeled and simulated in MATLAB. Simulation and experimental results are provided to demonstrate the effectiveness of the proposed control strategy for large-scale gridconnected cascaded PA full detailed model is described and its control scheme is designed. The dynamic performance of the designed architecture is verified by computer simulations and Further Extension can be done using Fuzzy Logic Controller.

I. INTRODUCTION

The present technology depends on renewable energy sources. In that mainly focused on PV System. The utilization of the grid connected Photovoltaic (PV) system can be increased being pursued as a supplement and an alternative to the conventional method of power generation to meet the energy demand. The major concentration of integrating PV system into the grid is stochastic behaviors of solar irradiations and interfacing of inverters with the grid in [1]. The Maximum power point tracking (MPPT) technique is widely used to extract maximum power from the PV system that is delivered to the grid through the inverter in [2]. THE modular multilevel converter (MMC) was introduced in 2002 [1] as dc–3ac configuration for high-voltage dc power transmission. The use of this topology for feeding electrical drives in the range of medium voltage was proposed in [2] and [3]. First, experimental results with low-voltage prototypes of MMC-based drive converters are shown in [4] and [5]. The most challenging issue of operating the MMC at low frequency, which is necessary for variable-speed drives, was first solved in [6]. The increasing amount of the energy pulsation in the capacitors of the cells at low frequencies or even standstill is reduced to acceptable values by the use of an ac commonmode voltage with corresponding inner currents. An appropriate control scheme, especially for this low-frequency mode, is presented in [7] and [8]. Here, a cascaded structure with subordinated current control loops and filter-based energy control loops is proposed. The optimization of the modulation [9] as well as the dimensioning process of the MMC [10] allow an efficient and high dynamic operation of the MMC for feeding three-phase machines. In [10] and [11], experimental results based on this control scheme and optimizations are shown. For an operation at nominal torque of the machine even at low frequencies, see [12], the MMC has to be overdimensioned with respect to the additional current stress of the inner balancing currents compared to the operating point at nominal speed. The authors of [12] proposed a new method for reducing the energy pulsation in the range of intermediate-speed and present extensive measuring results of steady-state operations at different frequencies. A further improvement for reducing the peak values of the inner currents by using square-wave currents for the balancing task is shown in [13]. This method causes large ac-contents in the dc voltage respectively in the dc current. A dynamic control of the MMC for feeding electric drives is proposedand demonstrated by experimental results. However, in [12], no waveform of the dc current is shown, which is also an important aspect regarding additional current stress of the dc-voltage source due to a possible harmonic content.

II. PHOTOVOLTAIC MODULE

Modelling is the basis for computer simulation of a real system. It is usually based on a theoretical analysis of the various physical processes occurring in the system and of all factors influencing these processes.. The most common model used to predict energy production in photovoltaic cell modelling is the single diode circuit model that represents the electrical behaviour of the pn-junction is given in fig 1 Figure shows how photovoltaic system works. The ideal photovoltaic module consists of a single diode.A solar cell is the building block of a solar panel. A photovoltaic module is formed by connecting many solar cells in series and parallel. Considering only a single solar cell; it can be modelled by utilizing a current source, a diode and two resistors. This model is known as a single diode model of solar cell
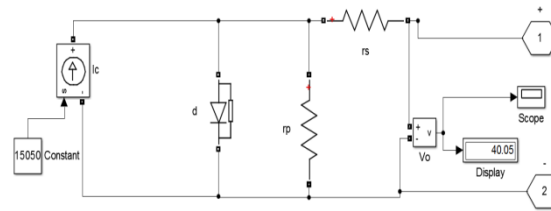
Figure 1: Single diode model of a solar cell

III.   Structure, Fundamentals, and Definitions of the MMC

The complete system including the dc-voltage source, the MMC itself, and the three-phase machine is illustrated in Fig. 1 [10]. The MMC includes three phases, each with an upper arm and a lower arm n. The currents in the arms are defined as ixy (upper or lower arm: $x \in \{p,n\}$, no. of phase: $y \in \{1, 2, 3\}$). One converter arm is built by m cells (no. of cell: $z \in \{1 \cdots m\}$) connected in series plus a coupled inductor L. One cell of this dc−3ac configuration consists of a single half bridge with a capacitor Cz . By switching the half bridges of the cells, each arm is able to generate an adjustable arm voltage uxy with m+1 voltage steps. Due to the half bridges in the cells and a pulsewidth modulation (PWM) of at least one cell, the range of the specific arm voltage
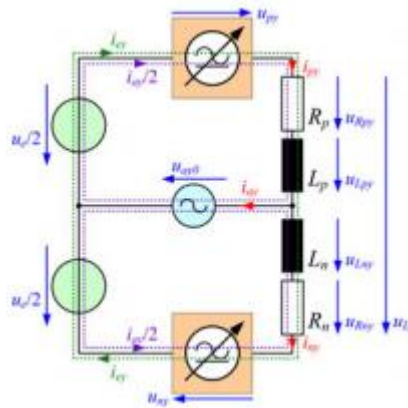

Fig.2 Equivalent circuit of one phase of the MMC

3.1. Function of the Arm Inductances

The inductances L decouple the six voltage sources realized by the arms of the MMC. In this approach, the inductances allow the individual adjustment of the several currents by the respective current control loops with the voltage components of (12) and (13). In [2] and [17], it is proposed to use the inductance for damping the internal currents in the range of the output frequency. This feature is not necessary by using the presented decoupled current control, because only the desired internal currents are adjusted and the arm voltages uxy are independently generated by the modulator [7], [10]. Therefore, the inductance L has to be dimensioned on the basis of the switching states of the cells and accordingly with the modulation scheme. In [10], the design process of the inductance is described in detail. To sum up, the inductance L is determined by the maximum allowed ripple content of the dc and inner currents Δiey . It depends on the switching frequency fPWM of the PWM, if one cell per arm and switching cycle is modulated, and on the cell voltage uCxyz . Consequently, the value of the inductance L is determined by the voltages on the level of the cells and not by the voltages or currents of the arms. This yields to a relative small value of the inductance L. To change the desired currents ie0 and ieα/β in the control loops, only small voltage components are necessary. Because of this, the parts of uLα/β/0 are neglected in Section III-A.

3.2. Current Control Loops of the MMC

 The three current control loops, see Fig. 4, for ieα , ieβ , and ie0 are derived by the equivalent circuits of Fig. 3 and their equations (11). Each control loop incorporates the impedances (L, R) of the arms, in which the current components have to be controlled by the corresponding voltages uLα , uLβ , and uL0 , see Fig. 3. The measured value of the dc voltage ue is used as feedforward in the control loop of ie0 , see Fig. 4.
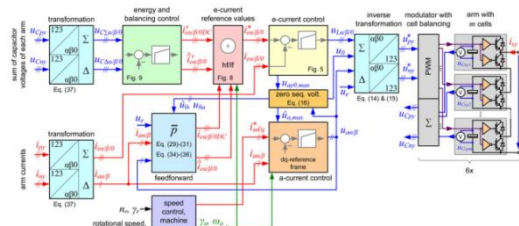
Fig.3 Signal flow path of complete MMC control system with subordinate current controllers, arm energy balancing, motor control unit, and modulator.
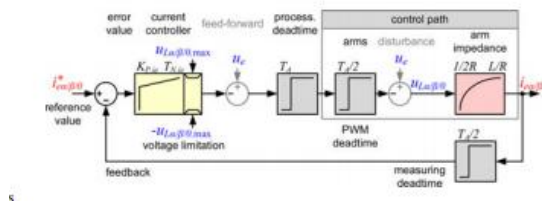

Fig.4 Current control loops of the e-currents in transformed components.

Each current controller is realized by a time-discrete P- or PI-controller (P: proportional, I: integral) with the sampling time TA . The dead times of the measurement, signal processing, and PWM are included by the sum of the small time constants Tσ,ie =2TA . Then, the maximum gain of the proportional part of the controller.

IV.   BALANCING OF THE ARM ENERGIES

The mean value of each power component $p^-\Sigma/\Delta\alpha/\beta/0$ has to be zero for a symmetrical energy distribution in steady-state operation, according to the desired constant value of the arm energy w^-C , see (3). Therefore, the specific currents and voltages for a directed influence on the transformed arm energies have to be identified by these transformed power components .Here, two methods of energy balancing have to be distinguished depending on the frequency ωa of the three-phase currentsiay . If ωa is high enough, which yields to the rotation of the phase angle by $\gamma a =\omega a \cdot t$ over the time t, only the mean values of the power components respectively the active power components have to be considered (high-frequency mode/hf mode). Consequently, the ac power components are buffered by the capacitors of the cells, which yields to the voltage pulsations $u^\sim Cxy$ in the arms. At lower output frequencies, the amount of the energy pulsation increases inversely proportional to ωa [1]. Because of this, a compensation of the instantaneous power components in the arms, which are caused by the three-phase load, is needed (low-frequency mode/lf mode) [6], [7]. This allows the stable operation of the MMC even at standstill respectively at frequency $\omega a =0$.

4.1. Horizontal Balancing: The energy transfer between the three phases of the MMC for the balancing in horizontal direction, see Fig. 5, is achieved by the dc-components of the inner currents $ie\alpha DC$ and $ie\beta DC$. They generate together with the dcvoltageue active power components in $p\Sigma\alpha$ and $p\Sigma\beta$. In each phase of the MMC occurs a dominant energy pulsation with the second harmonic of the output frequency ωa . This power component could be compensated by additional inner ac currents $ie\alpha,hf$ 2 and $ie\beta,hf$ 2 for reducing the energy pulsation in the arms (hf2-mode).

4.2. Mean Energy Control: The total energy stored in all cells of the MMC is influenced by the difference between the dc power and the 3ac active power Pa. The dc current for the power exchange with the dc-voltage source ue will be without losses.

4.3. Vertical Balancing: The vertical balancing task ensures energy equilibrium between the upper and lower arms of the MMC, see Fig. 5. The power components $\pm ua\alpha/\beta \cdot ie\alpha/\beta$ generate active power if the e-currents contain an ac current with the same frequency as $ua\alpha/\beta$. These methods can be used in the hf-mode, if the output frequency is high enough. The internal 3ac-current system is divided in its symmetrical components (positive and negative sequence components), [20], where D is the rotation matrix of (44) according to the phase angle γa.
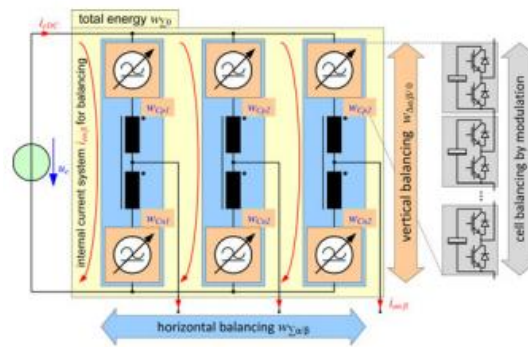
Fig.5 Energy control and balancing tasks in the MMC.

V.   CONTROL SYSTEM OF THE MMC FOR VARIABLE-SPEED DRIVES

The complete control system for the MMC drive system is illustrated in Fig. 3. The six sums of the capacitor voltages uCxy of each arm as well as the six-arm currents ixy are measured and transformed according to Section III-A to their related components, see Table I (here: $x \in \{uC ,i\}$)

$$\begin{bmatrix} x_{\Sigma\alpha} \\ x_{\Sigma\beta} \\ x_{\Sigma 0} \end{bmatrix} = \frac{1}{2} \mathbf{C} \cdot \begin{bmatrix} x_{p1}+x_{n1} \\ x_{p2}+x_{n2} \\ x_{p3}+x_{n3} \end{bmatrix} \qquad \begin{bmatrix} x_{\Delta\alpha} \\ x_{\Delta\beta} \\ x_{\Delta 0} \end{bmatrix} = \mathbf{C} \cdot \begin{bmatrix} x_{p1}-x_{n1} \\ x_{p2}-x_{n2} \\ x_{p3}-x_{n3} \end{bmatrix}.$$
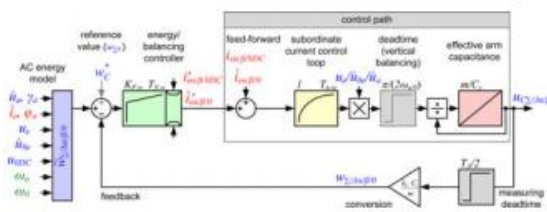

Fig.6 Effective control loop for balancing the arm energies of the MMC.

The five-current components are routed to their current controllers, which are described in Section II-D. The a-current controller of the three-phase machine receives its reference values in d- and q-components from its superposed speed controller. The machine model in the speed controller has to calculate the reference angle γa and the corresponding electrical frequency ωa for the dq-current controller as well as for the phase angles of the internal ac balancing currents. The control voltages of the current controller are converted to the reference values of the arm voltages u∗xy by the inverse transformation, see (14) and (15). The modulator (see block PWM in Fig. 7), which includes the cell balancing task, generates the pulse patterns for the transistors in the cells. The used modulation method is described in [7] and [10].

VI.   SIMULATION RESULTS

The process of the dimensioning of the MMC regarding the necessary cell capacitance Cz for buffering the pulsating energies in the arms as well as the resulting current stress are extensively described in [10]. A low-voltage MMC prototype, see [9] and [11], is designed based on these fundamentals to demonstrate the effectiveness of the control system for feeding three-phase machines. It consists of m=5 cells per arm with the maximum cell voltage of uCxyz,max =150 V and the cell capacitance of Cz =4400 μF. The MMC is supplied by a voltage source with ue =600 V and feeds a 15-kW threephase induction machine. The reference voltage of the energy controller is set to u⁻C =650 V. The measurements in Fig. 9 of the arm voltage up1 , of the corresponding arm current ip1 , as well as the voltage waveforms on the 3ac-side at the hf-mode demonstrate the high-quality waveforms with very low-harmonic content. The run-up of the field-orientated controlled induction machine is illustrated in the measurements of Fig. 8. The machine is magnetized by id and a step in the torque is initiated by iq at t=0.05 s. The fast dynamic response of the controlled MMC after this step causes no overshoot, neither in the currents nor in the capacitor voltages uCxy . During the low-speed operation of the machine, the MMC is balanced by the lf-mode until the mode is switched to the hf-mode in the range of t≈[0.5..0.7]s. This is

visible on the significant ac component of the commonmode voltage u0 and the corresponding inner balancing currents ieα/β . The magnitude of the energy pulsation in the lf-mode can be freely adjusted by ω0 . The choice of ω0 =2π × 100 Hz causes the desired effect in the capacitor voltages uCxy to keep them in the allowable range around the desired mean value of u¯C =650 V. The phase currents iay respectively iq and id are reduced during the lf-mode to keep the inner balancing currents ieα/β and, therefore, the arm currents ixy in acceptable limits. This is necessary, because the MMC is dimensioned on the basis of the current stress at the nominal operating point. During the switchover between the lf- and hf-mode, the motor currents are increased to their nominal values, because the additional current stress of the inner currents is decreased to nearly zero. The switchover between the lf- and hf-mode is set in the range of ωa1 =2π × 20 Hz and ωa2 =2π × 30 Hz. In the hf-mode, only a very small current ripple remains in the internal balancing currents due to the simplification of the calculated arm energies, where the control voltages are neglected. The dc-current ieDC obviously contains no ac component not even in the lf-mode.
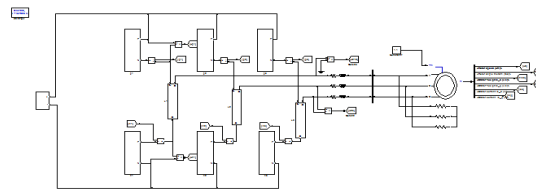

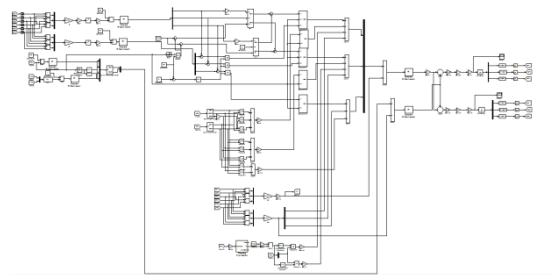Fig.7Proposed model of simulation diagram

Fig.8 simulation of Signal flow path of complete MMC control system with subordinate current controllers, arm energy balancing, motor control unit, and modulator.
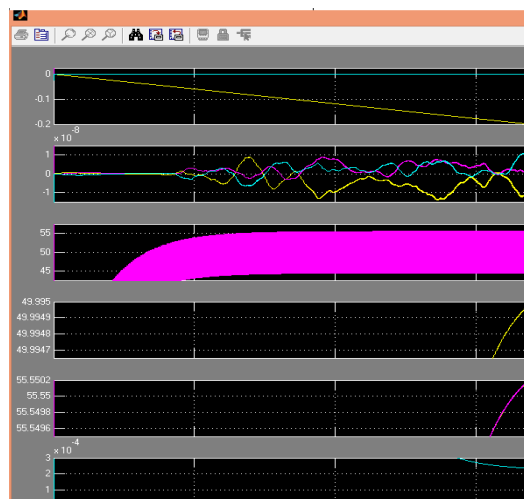

Fig.9 Run-up of a field-oriented controlled induction machine fed by the MMC prototype, short time averaged values at *TA* =1/*f*PWM =1/(8 kHz).

VII.   CONCLUSION

A cascaded control system for the MMC to feed variablespeed drives is derived on the base of the analysis of the equivalent circuit as well as of the active power components in the arms by using PV system. The realization by the transformation of all relevant values allows a dynamic control of the arm energies over the complete operation range of the drive at minimum internal currents. The systematically design process of the several

controllers and feed-forward components for the balancing tasks are presented. Finally, the measurement at a MMC prototype combined with

a field-oriented control of an induction machine validates the approach and illustrates the performance of the control system. The proposed control and balancing system of the MMC allows

the supply of three-phase machines independent of their type and motor control system.

REFERENCES

[1] R. Marquardt, A. Lesnicar, and J. Hildinger, "ModularesStromrichterkonzept fur NetzkupplungsanwendungenbeihohenSpannungen," ¨ presented at the ETG-Fachtagungen, Bad Nauheim, Germany, 2002.

[2] M. Hiller, D. Krug, R. Sommer, and S. Rohner, "A new highly modular medium voltage converter topology for industrial drive applications," in Proc. 13th Eur. Conf. Power Electron. Appl., 2009, pp. 1–10.

[3] M. Hagiwara, K. Nishimura, and H. Akagi, "A modular multilevel PWM inverter for medium-voltage motor drives," in Proc. IEEE Energy Convers. Congr. Expo., 2009, pp. 2557–2564.

[4] M. Hagiwara, K. Nishimura, and H. Akagi, "A Medium-Voltage Motor Drive With a Modular Multilevel PWM Inverter," IEEE Trans. Power Electron., vol. 25, no. 7, pp. 1786–1799, Jul. 2010.

[5] A. Antonopoulos, K. Ilves, L. Angquist, and H.-P Nee, "On interaction between internal converter dynamics and current control of highperformance high-power AC motor drives with modular multilevel converters," in Proc. IEEE Energy Convers. Congr. Expo., 2010, pp. 4293– 4298.

[6] A. Korn, M. Winkelnkemper, and P. Steimer, "Low output frequency operation of the Modular Multilevel Converter," in Proc. IEEE Energy Convers. Congr. Expo., 2010, pp. 3993–3997.

[7] J. Kolb, F. Kammerer, and M. Braun, "A novel control scheme for low frequency operation of the Modular Multilevel Converter," in Proc. Power Electron., Intell. Motion Energy Manag. Eur., 2011, pp. 977–982.

[8] J. Kolb, F. Kammerer, and M. Braun, "Straight forward vector control of the Modular Multilevel Converter for feeding three-phase machines over their complete frequency range," in Proc. 37th Annu. Conf. IEEE Ind. Electron. Soc., 2011, pp. 1596–1601.

[9] J. Kolb, F. Kammerer, P. Grabherr, M. Gommeringer, and M. Braun, "Boosting the efficiency of low voltage modular multilevel converters beyond 99%," in Proc. Power Electron., Intell. Motion Energy Manag. Eur., 2013, pp. 1157–1164.

[10] J. Kolb, F. Kammerer, and M. Braun, "Dimensioning and design of a Modular Multilevel Converter for drive applications," in Proc. 15th Int. Power Electron. Motion Contr. Conf., 2012, pp. LS1a-1.1-1–LS1a-1.1-8.

[11] J. Kolb, F. Kammerer, and M. Braun, "Operating performance of modular multilevel converters in drive applications," in Proc. Power Electron., Intell. Motion Energy Manag. Eur., Nuremberg, Germany, 2012, pp. 583– 590.

[12] A. Antonopoulos, L. Angquist, S. Norrga, K. Ilves, and H.-P. Nee,"Modular multilevel converter ac motor drives with constant torque form zero to nominal speed," in Proc. IEEE Energy Convers. Congr. Expo., 2012, pp. 739–746.